What is the best density functional to describe water clusters: Evaluation of widely used density functionals with various basis sets for (H2O)n (n = 1–10)

6 **AUTHORS**, INCLUDING:

Lu Wang
University of Science and Technology of Ch…
97 PUBLICATIONS   1,595 CITATIONS

SEE PROFILE

Jijun Zhao
Dalian University of Technology
390 PUBLICATIONS   8,424 CITATIONS

SEE PROFILE

Rui-Hua Xie
Xi'an Jiaotong University
154 PUBLICATIONS   1,698 CITATIONS

SEE PROFILE

Zhongfang Chen
University of Puerto Rico at Rio Piedras
220 PUBLICATIONS   7,995 CITATIONS

SEE PROFILE

REGULAR ARTICLE

What is the best density functional to describe water clusters: evaluation of widely used density functionals with various basis sets for (H$_2$O)$_n$ (n = 1–10)

**Fengyu Li · Lu Wang · Jijun Zhao ·
John Rui-Hua Xie · Kevin E. Riley ·
Zhongfang Chen**

Abstract The geometric structures, stabilization energies, dipole moments, and vibrational frequencies of the neutral water clusters (H$_2$O)$_n$, with n = 1–10, were investigated using density functional theory along with a variety of exchange-correlation functionals (LDA with SVWN5 parameterization, GGA with BLYP, PW91, PBE, B3LYP, X3LYP, PBE0, PBE1W, M05-2X, M06-2X and M06-L parameterizations) as well as high-level ab initio MP2 and CCSD(T) methods. Using the MP2 and CCSD(T) results as benchmarks, the effects of exchange-correlation functionals and basis sets were carefully examined. Each functional has its advantage in certain aspects; for example, M05-2X and X3LYP yield better geometries, and the capability of these two functionals to distinguish the relative energies between isomers are more similar to MP2. The size of the split-valence basis set (6-31G or larger), diffuse functions on the oxygen atom, and d(p) polarization on the oxygen (hydrogen) atom are crucial for an accurate description of inter-molecular interaction in water clusters. The 6-31+G(2d,p) basis set is thus recommended as a compromise between computational efficiency and accuracy for structural description. We further demonstrated that the numerical basis set, TNP, performs satisfactorily in describing structural parameters of water clusters.

Keywords Water cluster · Density functional theory · MP2 · CCSD(T) · Basis set · Structures · Relative energies · Stabilization energy · Dipole moment · Vibrational frequencies

F. Li · L. Wang · J. Zhao (✉)
School of Physics and Optoelectronic Technology, and College of Advanced Science and Technology, Dalian University of Technology, Dalian 116024, People's Republic of China
e-mail: zhaojj@dlut.edu.cn

F. Li
Department of Physics, University of Puerto Rico, San Juan, PR 00923, USA

J. R.-H. Xie
Department of Applied Physics, Xi'an Jiaotong University, Xi'an 710049, People's Republic of China

K. E. Riley
Institute of Organic Chemistry and Biochemistry, Academy of Sciences of the Czech Republic, Flemingovo nam. 1, Praha 6 16610, Czech Republic

K. E. Riley · Z. Chen (✉)
Department of Chemistry, Institute for Functional Nanomaterials, University of Puerto Rico, San Juan PR00923, USA
e-mail: zhongfangchen@gmail.com

1 Introduction

As a major chemical constituent on the Earth's surface, water is indispensible to all life. It is important to study water clusters, aggregates of water molecules held together by hydrogen bonds, in order to explain the formation of clouds and ice, solution chemistry, biochemical process, and many "anomalous" properties of water [1, 2]. Since many properties of clusters are size-dependent, significant experimental and theoretical efforts have been devoted to investigating the structural, energetic, vibrational, and other properties of water clusters as a function of cluster size.

Since the 1970s, various physical and chemical properties of very small water clusters have been measured experimentally. For the water dimer, Dyke et al. determined the geometric structure using microwave spectroscopy [3–5], whereas Curtiss et al. [6] quantified its binding energy and various thermodynamic properties. For water trimer, a chain-like configuration was first suggested by a matrix isolation vibrational spectroscopic study [7]; however, this assignment was challenged, and there was evidence for a cyclic structure in the gas phase [8–10] as well as inside matrix isolation [11]. For (H$_2$O)$_n$ clusters with $n = 3$–10, a series of spectroscopic investigations in molecular beams and rare-gas matrices revealed that the equilibrium configuration of each molecular cluster is closely related to the cluster size n [7–20]. For example, far-infrared vibration–rotation–tunneling and infrared laser spectroscopic studies conclusively demonstrated a cyclic structural pattern for (H$_2$O)$_n$ with $n = 3$–5 [13, 14, 18], a transition into a three-dimensional (3D) cage configuration at $n = 6$ [15], and other 3D structures for (H$_2$O)$_{7–10}$ [16, 17, 19, 20].

Theoretically, numerous ab initio computations have been well documented on the water clusters, with emphasis on the molecular structure, vibration frequency, binding energy [21–28], dipole moment [29–31], nuclear magnetic resonance parameters [32], isotope effect [33, 34], the effect of nanoscale confinement [35–38], structural transition under electric field [39, 40], as well as their protonated, hydroxylated, and ionic analogs [25, 41–47]. Water clusters have also been well investigated by means of empirical potentials. For example, Fang's group systematically simulated water transportation across biological and nanoscale channels and the wetting properties of the solid surfaces with nanoscale patterned structures [48–51].

Since the number of structural isomers increases dramatically with increasing cluster sizes, substantial efforts of quantum chemical computations have been given to compare the isomer energies [21, 25, 29, 52–56] and search for the global minima [57–59]. For instance, Kim et al. [21] thoroughly examined (H$_2$O)$_{4–8}$ isomers using the combination of the Metropolis Monte Carlo method and SCF computations, providing the basic skeleton of water clusters for many later studies. Besides the first-principles methods, empirical potentials such as ASP, MCY, SPC/E, and TIPnP ($n = 3$, 4, 5) were also frequently used to explore the potential energy surface of water clusters and locate the global minima [57–60].

Among those theoretical efforts, particular attention has been paid to the intermolecular hydrogen bonding interaction in water clusters. Using the second-order Møller–Plesset perturbation theory (MP2) [61], Xantheas et al.'s systematic computations obtained highly accurate interaction energies at the complete basis set (CBS) limit for (H$_2$O)$_n$ ($n = 2$–6) [23], which have often been used as benchmarks

for other methods [62]. Very recently, Shields et al. [63] proposed a simplified procedure to approach the MP2-CBS treatment for (H$_2$O)$_{2–10}$. However, for larger systems, MP2 computations become too computationally demanding.

Compared with the accurate but costly MP2 approach, DFT provides a compromise between computational accuracy and efficiency and has been employed to study a variety of hydrogen-bonded systems [25, 62, 64–83]. Despite the insufficient description of London dispersion forces [75], it is generally believed that DFT is able to yield results quantitatively comparable to those at the MP2 level of theory for water clusters, since hydrogen bonding comes mainly from electrostatic interaction and charge transfer that are easier to describe.

However, it has not been well established which is the most appropriate exchange-correlation functional for accurately describing the hydrogen bonding in liquid water [64, 80, 84], ice [71, 79], water/amino acid complexes [78, 81], and so on. For example, when describing the structural and dynamical properties of liquid water, Car–Parrinello molecular dynamics (CPMD) simulations using the BLYP functional reproduce the experimental data well [64]. The hybrid functionals (B3LYP, X3LYP, PBE0) perform even better than the pure functionals (BLYP, XLYP, PBE, rPBE), while LDA predicts strongly over-structured liquids [80]. The CPMD simulation with the BLYP functional on the isotropic average of the static distortions of ice-VI by Kuo and Kuhs [79] agrees with the indirect experimental estimation. The dispersion-enhanced density functionals recently developed by Truhlar's group [77, 85, 86] describe the non-covalent interacting systems including water clusters well [25, 54, 85, 87, 88].

The availability of both experimental and high-level theoretical data makes small water clusters ideal models to evaluate the performance of DFT methods in treating hydrogen-bonded water systems [22, 24, 64, 71, 75, 78–80, 89–94]. However, most of the previous studies only concentrated on small clusters (from monomer to hexamer) with limited numbers of structural isomers at each size. For example, Anderson and Tschumper pointed out that 10 different functionals (X3LYP, B3LYP, B971, B98, MPW-LYP, PBE1PBE, PBE, MPW1 K, B3P86, and BHandH-LYP) provide reliable geometrical parameters and relative energies of water dimers with regard to the CCSD(T) references [24]. Kim and Jordan demonstrated that the B3LYP functional reasonably reproduces the MP2 data for the water monomer and dimer [22]. Dahlke and Truhlar [91] carefully examined the accuracy of 25 functionals with several basis sets for describing non-covalent interaction energies in water dimers and trimers, and PBE1W was found to have the smallest mean unsigned error. Csonka et al. [75] searched for the appropriate Gaussian basis sets for DFT (B3LYP, X3LYP, PBE1W and B971)

computations of water dimers and trimers. Santra et al. [92] assessed 16 functionals in treating water clusters from dimer to pentamer and found that PBE0 and X3LYP perform best for the energetics of the H bonds. Recently, Bryantsev et al. [25] found that the M06-class functionals give more accurate binding energies for neutral, protonated, and deprotonated water clusters $(H_2O)_n$ ($n = 1$–6).

Since only a limited number of isomers for small clusters were considered in earlier efforts, it is still desirable to further evaluate the performance of DFT methods for water clusters, to include the new-generation functionals, to extend the number and size of water clusters in the dataset, and to more systematically examine the capabilities of DFT for comprehensive property analyses of water clusters, which are far easier to understand than the bulk systems [54]. Moreover, it is also critical to find the "optimal basis set" with both sufficiently high accuracy and efficiency.

In this paper, using MP2 or CCSD(T) as benchmarks, we evaluated the performance of 11 widely used DFT functionals to model the structures, electronic properties, and relative energies of water clusters up to the decamer. The effect of basis sets was also examined. These efforts should be beneficial for choosing the appropriate computational methods in the simulation of larger water clusters as well as bulk water systems of different morphologies.

2 Computational methods

The majority of the present ab initio computations were performed using the Gaussian 09 program [95] with either MP2 or DFT methods. In addition, the DMol^3 program [96, 97] was used to assess the double numerical set plus polarization functions (DNP) basis set, and the triple numerical set plus polarization function (TNP). All the cluster configurations were fully optimized without any symmetry constraint and were characterized as local minima by frequency analysis.

A variety of "popular" functionals for the exchange-correlation interactions were examined, including the local density approximation (LDA) with SVWN5 [98] parameterization, the "pure" generalized gradient approximation (GGA) with BLYP [99], PBE [100], PW91 [101], and PBE1W parameterizations, the hybrid GGA with PBE0 [102], B3LYP [103], and X3LYP [104] parameterizations, and the dispersion-enhanced GGA with M05-2X [85], M06-2X [88], and M06-L [86] parameterizations. Meanwhile, reference MP2 computations were carried out in order to judge the quality of the DFT methods. All DFT computations were done with the same MG3S basis set, i.e., 6-311+G(2df,2p) [105], and the MP2 method was used along with the 6-311++G(2d,2p) basis set.

To examine the reliability of the reference data, namely MP2/6-311++G(2d,2p) results, we employed CCSD(T) [106–108] with the aug-cc-pVTZ basis set implemented in the MOLPRO program [109] to investigate the small $(H_2O)_{1-6}$ clusters. Since the mean deviation of structural parameters (O–H and O–O distances) of MP2/6-311++G (2d,2p) to CCSD(T)/aug-cc-pVTZ is less than 0.003 Å for $(H_2O)_{1-3}$, we carried out CCSD(T)/aug-cc-pVTZ single-point energy computations based on MP2/6-311++G (2d,2p) optimized geometries for $(H_2O)_{4-6}$ clusters. The mean deviation of relative energies of $(H_2O)_{4-6}$ between CCSD(T)/aug-cc-pVTZ and MP2/6-311++G(2d,2p) results is only 0.11 kcal/mol, demonstrating that MP2/6-311++G(2d,2p) qualifies as a suitable reference to judge the performance of DFT methods.

We also investigated the effect of basis sets on the description of various properties of water clusters. First, we chose a series of basis sets of different sizes, i.e., 6-31+G(2df,2p) and 6-311+G(2df,2p). Second, the effects of polarization functions were examined by comparing the 6-31G+(2d,2p), 6-31+G(2d,p), 6-31+G(d,p), 6-31+G(d) basis sets.

Typically, basis set superposition error (BSSE) is taken into account for small water clusters, here we concentrate on finding a suitable functional to reproduce the structures and relative energies of small water clusters by MP2, so as to further investigate large water clusters and to gain insight into the structural evolution from individual water molecule to bulk water. Therefore, no counterpoise corrections [110] were used.

On the other hand, it has been observed that the inclusion of zero-point energies (ZPE) can change the relative order of water clusters [54, 111, 112]. Notably, for water hexamers, the relative energies between isomers at the MP2 and DFT levels of theory only deviate slightly (~0.1 kcal/mol) from those at the CCSD(T) level, regardless of whether the ZPE corrections are included or not [54]. Since we mainly consider the relative energies of the water clusters, ZPE corrections were not included in our computations.

3 Results and discussion

3.1 Performance of DFT functionals with regard to experimental and high-level theoretical data (mainly MP2)

3.1.1 Geometries, dipole moments, stabilization energies, and vibrational frequencies of the water monomer and dimer

The water monomer and dimer have frequently been used as benchmarks to evaluate different theoretical methods [22, 24, 75, 91, 113] since experimental data are available for

comparison. Table 1 summarizes the geometric parameters, stabilization energies, dipole moments, and vibrational frequencies for the water monomer and dimer obtained at the CCSD(T), MP2, and DFT levels of theory, along with the experimental data [3, 4, 6, 114–118]. MP2 and all DFT computations were done with the 6-311++G(2d,2p) and MG3S basis sets, respectively, while the CCSD(T) computations employ the aug-cc-pVTZ basis set.

3.1.1.1 Water monomer The GGA methods tend to overestimate the O–H distance [119, 120] compared with experiment, which is also verified by our computations. However, computations with the dispersion-enhanced functionals (M06-L, M06-2X), as well as PBE0 and MP2 methods, yield the exact O–H bond length. The H–O–H bond angle predicted by BLYP (104.60°) is closest to the experiment (104.52°), while the values from CCSD(T), MP2, M06-L, PBE, PBE1W and PW91 calculations (104.18°–104.37°) are slightly smaller.

The dipole moment of a molecule provides a quantitative measure of the electron distribution. Compared with the experimental data (1.854 Debye) [114], MP2 always yields larger dipole moments (2.06 Debye, see Ref. [22]), regardless of the basis set size. Similarly, all the density functionals used here overestimate the dipole moment of the water monomer by 4.3–8.7%, among these, the BLYP, PBE, PBE1W and PW91 functionals along with the MG3S basis set yield the value (1.93 Debye) closest to the experiment.

Generally, all the computational methods, including CCSD(T), MP2, and DFTs, overestimate the vibrational frequencies, and the scaling factor is method- and system dependent. The X3LYP computed vibrational frequencies (1,632, 3,826, and 3,929 cm^{-1}) agree best with the measured values (1,648, 3,832, 3,943 cm^{-1}) [116]; B3LYP's vibrational frequencies are closest to the CCSD(T)/aug-cc-pVTZ results; with the exceptions of MP2 and the dispersion-enhanced M-class functionals, the other functionals underestimate the vibrational frequencies compared with experimental values, especially the LDA and pure GGA functionals yield low vibrational frequencies.

3.1.1.2 Water dimer The intermolecular hydrogen bond in the water dimer can be characterized by the O–O distance. Here, we use the experimental value (2.976 Å) as the reference to judge different theoretical methods. It has been shown that MP2 slightly overestimates hydrogen bonding and thus shortens O–O distances to a small extent, while B3LYP and BP86 predict even shorter O–O distances than MP2 [22]. The same trend was revealed in this work: when combined with the MG3S basis set, all the functionals underestimate the O–O distances by up to 8.7%, BLYP (O–O distance 2.948 Å) agrees best with

the experimental data, followed by PBE1W (2.928 Å) and M05-2X (2.922 Å). Previously, Parrinello's group carried out quantum molecular dynamics simulations of liquid water and found that the BLYP method can reproduce the experimental radial distribution function rather well [64].

All the functionals considered here match the experimental dipole moment well. M06-L M06-2X, PW91, PBE, and PBE1W underestimate the dipole moment (experimental value 2.60 Debye [3]) by <1.54% (2.54–2.56 Debye), while other tested functionals like BLYP, B3LYP, X3LYP, PBE0, and LDA overestimate within 3.46% (2.61–2.69 Debye). M05-2X reproduces the experimental value (2.60 Debye), and PBE0 yields the second best results (2.61 Debye).

When the vibrational frequencies are concerned, we only considered the four most studied high-frequency O–H stretching modes, two of which involve O⋯H hydrogen bonds. Again, all functionals, excepting the M05 and M06 classes, predict smaller frequencies than MP2. Among all the functionals considered, the hybrid functionals prevail both pure and dispersion-enhanced DFTs, and B3LYP yields the best agreement (3,709, 3,814, 3,896, 3,914 cm^{-1}) with the experimental values (3,718, 3,797, 3,881, 3,899 cm^{-1}) [117, 118], followed by X3LYP, which gives similar values. Among the pure functionals, PBE, PBE1W, and PW91 behaves comparably, while BLYP performs worst, consistent with its insufficient description of the water monomer and dimer. Similar to the case of water monomer, B3LYP yields the frequencies that are closest to the CCSD(T)/aug-cc-pVTZ vibrational data. Among the dispersion-enhanced functionals, M06-L yields the values (3,725, 3,843, 3,946, 3,953 cm^{-1}) that are closest to the best ab initio predictions (3,750, 3,827, 3,914, 3,934 cm^{-1} [117]), followed by M06-2X and M05-2X.

The stabilization energy (SE) is also a crucial quantity to measure the intermolecular hydrogen bond strength in a water cluster. In this work, the stabilization energy per molecule for a water cluster containing n water molecules was calculated via the following definition:

$$SE(n) = -(E_n - nE_1)/n, \qquad (1)$$

where E_n represents the total energy of entire cluster, and E_1 is the total energy of a water monomer. According to this definition, a positive SE value denotes that the formation of the water cluster is exothermic, while a negative one means that it is energetically unfavorable. The SE of the water dimer has been intensively investigated both experimentally and theoretically. The experimentally measured SE is 2.72 ± 0.35 kcal/mol per water molecule [6], while the high-level CCSD(T)/CBS [25] and MP2/CBS computations [23] predicted SE values of 2.51 and 2.49 kcal/mol, respectively.

Table 1 Geometric parameters, dipole moments (μ), stabilization energies (SE), and vibrational frequencies (v) of water monomer and dimer computed with CCSD(T), MP2, and 11 different exchange-correlation functionals

	Expt.	CCSD(T)[a]	MP2	M06-L	M06-2X	M05-2X	B3LYP	X3LYP	PBE0	BLYP	PBE	PW91	PBE1W	LDA
H_2O														
R_{O-H} (Å)	0.958 [112]	0.962 (0.959)	0.958	0.958	0.958	0.957	0.961	0.960	0.958	0.971	0.969	0.968	0.969	0.970
θ_{H-O-H}(°)	104.52 [112]	104.18 (104.16)	104.27	104.27	105.21	105.60	105.14	105.20	104.91	104.60	104.23	104.37	104.37	105.03
μ (Debye)	1.85 [3]	1.99	2.07	1.94	1.98	2.01	1.96	1.97	1.96	1.93	1.93	1.93	1.93	1.99
v (cm⁻¹)	1,648 [116]	1,646 (1,659)	1,660	1,666	1,627	1,617	1,632	1,632	1,639	1,599	1,598	1,599	1,596	1,552
	3,832	3,810 (3,833)	3,862	3,856	3,890	3,890	3,817	3,826	3,878	3,678	3,718	3,723	3,724	3,728
	3,943	3,919 (3,943)	3,982	3,971	3,994	3,990	3,920	3,929	3,984	3,781	3,825	3,829	3,832	3,838
R_{O-O} (Å)	2.976 [4]	2.914 (2.909)	2.917	2.907	2.900	2.922	2.920	2.905	2.890	2.948	2.879	2.880	2.928	2.721
μ (Debye)	2.60 [5]	2.67	2.78	2.56	2.56	2.60	2.68	2.69	2.61	2.62	2.54	2.56	2.55	2.61
$(H_2O)_2$														
v (cm⁻¹)	3,718 [117]	3,730 (3,750)	3,768	3,731	3,810	3,814	3,709	3,713	3,750	3,555	3,563	3,560	3,585	3,442
	3,797 [118]	3,805 (3,827)	3,852	3,844	3,886	3,899	3,814	3,820	3,871	3,672	3,712	3,717	3,718	3,711
	3,881	3,889 (3,914)	3,951	3,951	3,977	3,986	3,896	3,902	3,956	3,750	3,795	3,799	3,799	3,803
	3,899	3,911 (3,934)	3,968	3,957	3,987	3,994	3,914	3,920	3,974	3,772	3,815	3,820	3,821	3,816
SE (kcal/mol)	2.72 ± 0.35 [6]	2.61	2.63	2.47	2.80	2.76	2.48	2.68	2.70	2.30	2.77	2.95	2.76	4.63

The 6-311++G(2d,2p) and MG3S basis sets were used respectively for MP2 and DFT computations, while the aug-cc-pVTZ basis set was employed in CCSD(T) computations

[a] The values in parentheses are taken from Ref. [112], using CCSD(T)/TZ2P(f,d)+dif method

When compared with the experimental value (2.72 ± 0.35 kcal/mol), LDA significantly overestimates the SE value (4.63 kcal/mol) (see Table 1); among the GGA functionals, PW91 yields the largest SE (2.96 kcal/mol), while BLYP gives the lowest SE (2.30 kcal/mol); the hybrid PBE0 and X3LYP results (2.70 and 2.68 kcal/mol, respectively) well reproduce the experimental data. In 2004, Xu and Goddard [113] argued that X3LYP prevails for binding energy evaluation in such hydrogen-bonded systems among a variety of density functionals, which is further supported by our computations.

When the high-level CCSD(T) and MP2 CBS data are used as references (2.51 and 2.49 kcal/mol, respectively), M06-L and B3LYP give the best agreement (2.47 and 2.48 kcal/mol, respectively). MP2/6-311++G(2d,2p) gives 2.63 kcal/mol, very close to the CCSD(T)/aug-cc-pVTZ value of 2.61 kcal/mol.

Note that the MG3S basis set we used above is sufficient to give reliable results for SE predictions. The aug-cc-pVTZ basis set was confirmed to roughly give converged results for geometry optimization and thermochemical energies of water clusters [121]. The SE values computed at the MP2/6-311++G(2d,2p), B3LYP/MG3S, and BLYP/MG3S levels of theory (2.63, 2.48, and 2.30 kcal/mol, respectively) agree reasonably well with those obtained by single-point energy computations (2.6, 2.3, and 2.1 kcal/mol, respectively) using the larger aug-cc-pVTZ basis set at the same level of theory (based on the same B3LYP/aug-cc-pVTZ optimized geometry) [122].

The thorough analyses described above on the water monomer and dimer lead to the following conclusions: (a) the hybrid GGA (PBE0, B3LYP, and X3LYP) are reasonably reliable for describing various aspects of the small water clusters; (b) among the pure GGA functionals considered, BLYP gives the best performance for structural description and dipole moments, but is less accurate for predicting SE; (c) the meta-GGA functional M06-L gives the best results while the other two dispersion-enhanced functionals considered also give reasonable results.

3.1.2 Structures and relative energies of $(H_2O)_n$ $(n = 2–10)$

For the larger water clusters with $n \geq 3$, very scarce experimental data exist for the geometries, dipole moments, and intermolecular interaction energies. Previous reports showed that MP2 can describe such hydrogen-bonded systems rather accurately [34, 123], and our current studies demonstrated that MP2/6-311++G(2d,2p) can give comparable structural and energetic data to CCSD(T)/aug-cc-PVTZ, thus we chose high-level MP2 results to calibrate different DFT methods in this work.

Starting from $n = 4$, there are several structural isomers for each cluster size. All isomers for the $(H_2O)_n$ clusters ($n = 2–10$) considered here are shown in Fig. 1. For a $(H_2O)_n$ cluster with n molecules, we respectively labeled the ground state configuration and the metastable isomers as "wn-0", "wn-1", "wn-2", and so on.

3.1.2.1 Predicting the lowest-energy isomer With the exception of $(H_2O)_6$, our computations revealed that MP2 and most DFT methods predict the same ground state structures for each cluster size, i.e., cyclic rings for $(H_2O)_4$ and $(H_2O)_5$, an edge-capped trigonal prism for $(H_2O)_7$, a cube with S_4 symmetry for $(H_2O)_8$, an edge-capped distorted cube for $(H_2O)_9$, and a pentagonal prism for $(H_2O)_{10}$, respectively. For $(H_2O)_6$, only the dispersion-enhanced functionals (M05-2X, M06-2X, M06-L) and LDA agree with MP2 predicting the lowest-energy hexamer isomer with a trigonal prism configuration. PW91, PBE, PBE1W, and PBE0 prefer the book structure, while B3LYP, X3LYP, and BLYP show that the ring-like hexamer is most energetically favorable.

The present results are generally consistent with previous studies [7–13, 15–20, 36, 53, 54, 124], except that there are some controversies [56] on the lowest-energy structure of the water hexamer. For example, Liu's experiments revealed that a cage-like structure is favorable for $(H_2O)_6$ [15], meanwhile a cyclic configuration was observed in Nauta and Miller's experiment [125]; on the other hand, the CCSD(T) calculations with or without BSSE show that the prism structure is the most stable [54]. In this subsection, we concentrate on the lowest-energy cluster configurations at each size, optimized by both MP2/6-311++G(2d,2p) and DFT methods with the MG3S basis set. The structural differences between MP2 and DFT methods will be discussed in the following subsection.

3.1.2.2 Structural properties of the lowest-energy $(H_2O)_{2–10}$ The structural properties of a water cluster can be characterized by the average adjacent O–O distance $\bar{R}_{O–O}$, which has been plotted as function of cluster size n in Fig. 2. For the smaller planar clusters ($n = 2–5$), $\bar{R}_{O–O}$ decreases with increasing cluster size due to enhanced intermolecular interactions; going from the dimer to the pentamer, both MP2 and DFT computations predict a shortening of O–O distances by ~ 0.2 Å, in agreement with the previous high-level MP2/aug-cc-pVTZ calculations [92]. Notably, a rapid rise of the $\bar{R}_{O–O}$ distance appears at $(H_2O)_6$ (Fig. 2), which corresponds to a transition from two-dimensional (2D) to three-dimensional (3D) configurations (see Fig. 1). However, only M06-L predicts the $\bar{R}_{O–O}$ distance of the prism hexamer to be shorter than that of the ring pentamer. For those larger 3D clusters, the O–O

Fig. 1 Structures of low-energy isomers for $(H_2O)_n$ clusters ($n = 2$–10) considered in this work. *White* and *red balls* denote hydrogen and oxygen atoms, respectively. The *dashed lines* represent hydrogen bonds
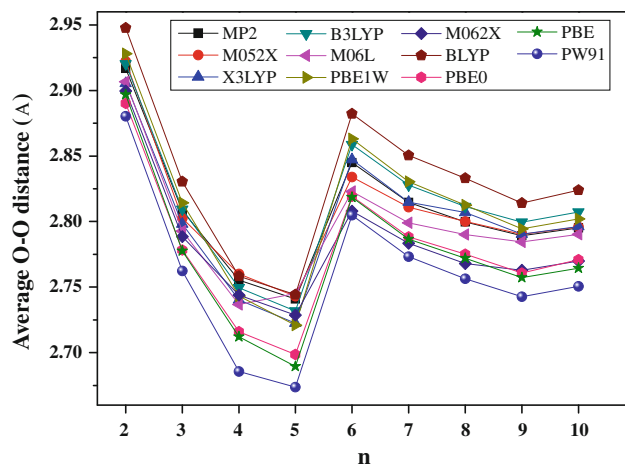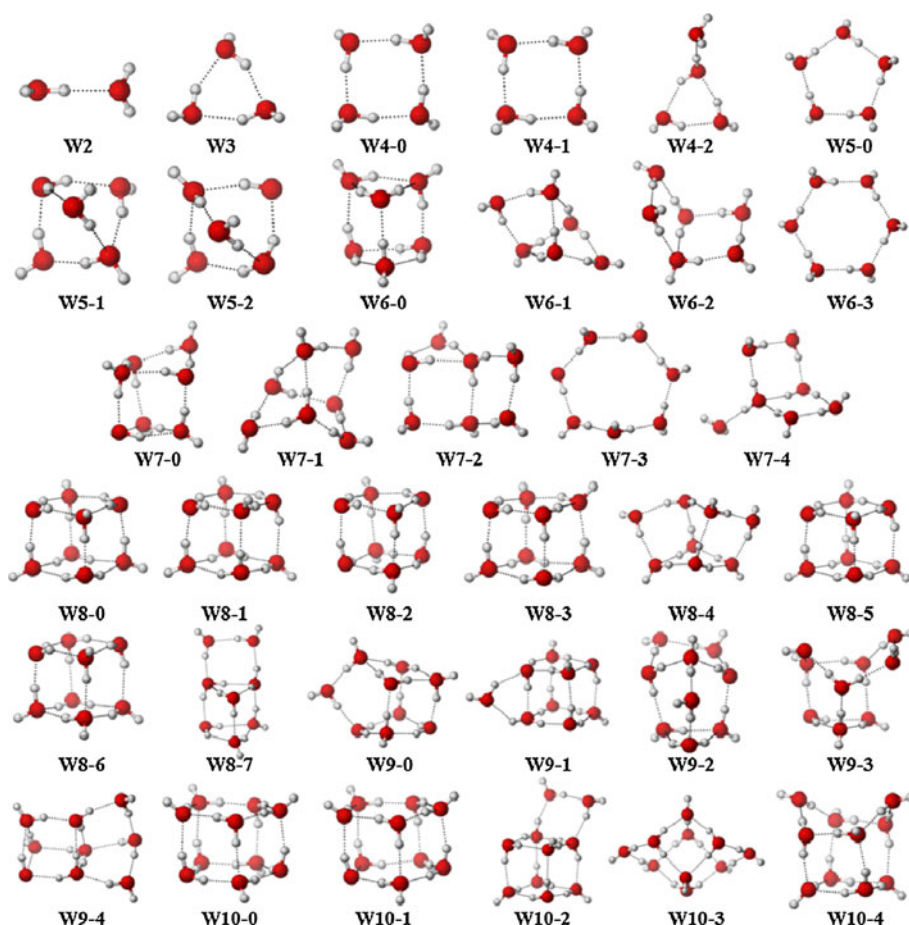

Fig. 2 Average adjacent O–O distance using MP2 method and 11 different exchange-correlation functionals with the MG3S basis set. The root-mean-squared deviation (RMSD) with regard to MP2 results is 0.004, 0.007, 0.009, 0.012, 0.012, 0.024, 0.024, 0.030, 0.032, 0.048, and 0.222 Å, for M05-2X, X3LYP, B3LYP, M06-L, PBE1W, M06-2X, BLYP, PBE0, PBE, PW91, and LDA, respectively. The O–O distance curve of LDA was not shown in the plot, since the LDA results deviate too much from the MP2 results

distance becomes less sensitive to the cluster size and reduces only slightly with n, with changes within the range of 2.74–2.85 Å. For comparison, the experimental O–O distance is 2.74 Å in ice [126] and 2.82 Å in liquid water [127], respectively.

For the water trimer, Keutsch et al. [128] provide an overview of the extensive literature, covering both theoretical studies and experimental observations. The experimental O–O distances of the water trimer from the vibration–rotation–tunneling spectroscopy are 2.97 and 2.94 Å [13]. Our computations using different methods underestimate the O–O distance by 0.06–0.14 Å. Among them, BLYP gives the value closest to the experimental one, while LDA performs worst.

Within the entire size range of $n = 2$–10, the M05-2X results are closest to the MP2 ones among all functionals examined. X3LYP yields the next closest results, and it is the only functional here that overestimates ($\sim 0.3\%$) the O–O distances, when compared with MP2 results, whereas the performance of B3LYP is also reasonably good. Though most of other functionals can reproduce the size-dependent trend of $\overline{R}_{O-O}$, their deviations from the MP2

Table 2 RMSD (in Å) of $\bar{R}_{O-O}$ of the 11 functionals with MG3S basis set compared with MP2/6-311++G(2d,2p) geometries for $(H_2O)_{4-10}$ clusters

	M05-2X	M06-2X	M06-L	X3LYP	B3LYP	PBE0	PBE1W	PBE	BLYP	PW91	LDA
$n = 4$	0.031	0.014	0.011	0.012	0.005	0.035	0.010	0.039	0.013	0.988	0.218
$n = 5$	0.012	0.015	0.013	0.007	0.010	0.032	0.013	0.038	0.021	0.052	0.228
$n = 6$	0.005	0.025	0.012	0.009	0.010	0.034	0.013	0.039	0.008	0.053	0.227
$n = 7$	0.003	0.020	0.564	0.007	0.009	0.032	0.008	0.037	0.016	0.051	0.219
$n = 8$	0.004	0.026	0.011	0.006	0.011	0.022	0.014	0.030	0.025	0.044	0.233
$n = 9$	0.004	0.020	0.702	0.006	0.016	0.022	0.013	0.025	0.030	0.041	0.223
$n = 10$	0.003	0.024	0.005	0.002	0.011	0.025	0.007	0.031	0.028	0.045	0.228
Average	0.009	0.021	0.188	0.007	0.010	0.029	0.011	0.034	0.020	0.182	0.225

values are relatively large. For example, PW91 systematically underestimates by $\sim 1.7\%$, the worst case is LDA, which even underestimates by $\sim 7.9\%$.

3.1.3 Distinguishing the $(H_2O)_n$ (n = 4–10) structural isomers

The study of water clusters holds considerable promise for obtaining molecular level insight into bulk water, since many of these isomers are reminiscent of the transient structures that appear in liquid water, and some clusters can be viewed as building blocks for the tetrahedral network of ice. A large water cluster has numerous locally stable isomers lying on the potential energy surface with very similar energies. Thus, it is crucial to examine the performance of the DFT functionals in distinguishing the structural isomers, which can be characterized by two factors: the geometry description and the energy differences between the ground state and the metastable isomers. The two features are discussed in the following.

The average adjacent O–O distances are addressed for the structural description. The root-mean-squared deviation of $\bar{R}_{O-O}$ for $(H_2O)_{4-10}$ clusters are listed in Table 2. Generally, all the DFT methods considered, with the exception of LDA, give satisfying geometries. The performance of any given functional varies at different cluster sizes. For example, as the cluster size increases, M05-2X gives very close geometries to MP2 results ($n = 6$–10), PBE1W yields the best structural parameters among the pure GGAs, while BLYP exhibits larger deviations from MP2 data. X3LYP shows the best overall performance, M05-2X gives the second best structural parameters, and LDA performs worst.

To differentiate the cluster isomers quantitatively, for each $(H_2O)_n$ cluster, we computed the energy difference $\Delta_{ni}^{functional}$ between the most stable configuration wn-0 and the other isomers wn-i ($i = 1, 2,…$) using different methods (MP2, M06-L, M05-2X, M06-2X, B3LYP, X3LYP, PBE0, BLYP, PBE, PW91, and LDA) along with the

MG3S basis set. Taking the MP2/6-311++G(2d,2p) results as standard, we defined a mean square deviation $\delta_n^{\text{Functional}}$ for each DFT functional at a given cluster size n:

$$\delta_n^{\text{Functional}} = \frac{1}{m} \sum_{i=1}^{m} \left| \Delta_i^{\text{Functional}} - \Delta_i^{\text{MP2}} \right|, \tag{2}$$

where m is the total number of metastable isomers at each cluster size. The overall deviation of each functional from the MP2 reference is obtained by averaging the $\delta_n^{\text{Functional}}$ for the seven cluster sizes ($4 \leq n \leq 10$) considered,

$$<\delta>^{\text{Functional}} = \frac{1}{7} \sum_{n=4}^{10} \delta_n^{\text{Functional}}. \tag{3}$$

With the above definitions, the $<\delta>^{\text{Functional}}$ can roughly measure the capability for a functional to distinguish the isomers of the water clusters.

Table 3 summarizes the $\delta_n^{\text{Functional}}$ and $<\delta>^{\text{Functional}}$ for each functional. Among all the functionals we studied, PBE0 gives the best description of the relative energies of the water clusters considered here (with an average deviation of 0.782 kcal/mol from the MP2 reference), the performance of M05-2X is comparable to PBE0 (with an RMSD of 0.787 kcal/mol), followed by M06-L and B3LYP (with RMSD values of 0.849 and 0.989 kcal/mol, respectively). Not surprisingly, LDA gives the worst performance. Notably, the energy of a water cluster is sensitive to the direction and arrangement of hydrogen bonds. Such effects are rather apparent for the water octamer isomers considered in this work. M05-2X outperforms in predicting the relative energies of the six cubic $(H_2O)_8$ structures (with an RMSD of 0.029 kcal/mol), followed by PBE (with an RMSD of 0.096 kcal/mol), while PBE0 deviates to a certain extent (with an RMSD of 0.116 kcal/mol) compared with MP2 data.

The main conclusion in this subsection is summarized as following: M05-2X is distinguished in describing both geometry parameters and relative energies among the three

Table 3 The RMSD of $(H_2O)_n$ isomer energies for $n = 4$–10 at the DFT level of theory with 11 different exchange-correlation functionals accompanied with MG3S basis set from those at MP2/6-311++G(2d,2p) level

	M05-2X	PBE0	X3LYP	M06-L	M06-2X	B3LYP	PBE	PBE1W	PW91	BLYP	LDA
$\delta_4^{Functional}$	0.206	0.299	0.239	0.209	0.275	0.131	0.561	0.294	0.252	0.144	2.966
$\delta_5^{Functional}$	0.994	1.132	2.542	1.543	1.679	1.450	2.753	2.635	2.924	1.743	0.258
$\delta_6^{Functional}$	1.258	0.988	1.237	1.368	1.883	1.564	1.238	1.405	1.329	2.083	1.506
$\delta_7^{Functional}$	0.661	0.981	1.267	0.952	1.222	1.689	0.879	1.299	0.813	2.468	2.672
$\delta_8^{Functional}$	0.263	0.115	0.125	0.395	0.446	0.265	0.180	0.199	0.254	0.359	2.515
	(0.029)	(0.116)	(0.103)	(0.270)	(0.284)	(0.185)	(0.096)	(0.202)	(0.107)	(0.299)	(1.532)
$\delta_9^{Functional}$	1.940	1.415	1.358	1.258	2.455	1.261	1.833	1.599	1.995	1.384	6.537
$\delta_{10}^{Functional}$	0.189	0.541	0.520	0.219	0.479	0.563	0.606	0.627	0.661	0.640	1.936
$<\delta>^{Functional}$	0.787	0.782	1.041	0.849	1.206	0.989	1.150	1.151	1.175	1.260	2.627

The data in parentheses denote the RMSD of six cubic octamer isomers

dispersion-enhanced functionals; X3LYP and PBE0 (respectively) yield good results on structural computations and relative energies among the hybrid GGA functionals; As for the non-hybrid GGA functionals, PBE1W gives slightly better performance, while the overall performances of other pure GGA functionals like PW91, PBE, and BLYP are comparable and acceptable.

3.2 Effects of split-valence basis sets

Few efforts have been made to examine basis set effects in different hydrogen-bonded systems [75, 104, 129, 130]. Here, we further explore basis set effects on the structural description of water clusters; in this study, we test the performance of the 6-31G and 6-311G basis sets, implemented with different levels of diffusion and polarization functions. The X3LYP functional was chosen as a representative for popular DFT methods since the above discussion shows that it is closest to MP2 results in the structural description of water clusters.

Again, we started from the water monomer and dimer, which have experimental data available. The results of X3LYP calculations for the water monomer and dimer employing two basis sets 6-311+G(2df,2p) and 6-31+G(2df,2p) are summarized in Table S1. For both monomer and dimer, the geometry parameters and dipole moments computed with the 6-311+G(2df, 2p) basis set at the X3LYP level agree well with the experimental values, whereas the performance of 6-31+G(2df,2p) basis set is already satisfactory.

We further considered the effects of diffuse and polarization functions, and the theoretical data are listed in Table S1. Csonka et al. [75] noted that the inclusion of diffuse functions in the oxygen basis set is very important. Here, we compared the performance of 6-31+G(2df,2p), 6-31+G(2d,2p), 6-31+G(2d,p), and 6-31+G(d) basis sets

in combination with the X3LYP functional. As shown in Table S1, 6-31+G(2d,2p) and 6-31+G(2d,p) can yield reasonable results that are comparable to 6-311+G(2df,2p), while 6-31+G(d) fails to reproduce the results of 6-311+G(2df,2p). Note the OH bond length and dipole moments are sensitive to the d(p)-polarized functions. We also examined the performance of the 6-31+G(2d,p) basis set in a wider size range, i.e., $n = 2$–10. The RMSD of $\bar{R}_{O-O}$ is 0.011 Å and confirms the conclusions drawn from the water monomer and dimer: 6-31+G(2d,p) is a good choice with decent accuracy and a reasonable computational cost.

Since M05-2X gives reliable relative energies and consistently predicts the lowest-energy structures ($n = 4$–10) with respect to MP2 results, we carried out M05-2X/MG3S single-point energy calculations based on X3LYP/6-31+G(2d,p) geometries, and the RMSD of relative energies is 0.848 kcal/mol, which is comparable with M05-2X/MG3S results (with the RMSD of 0.787 kcal/mol). Hence, we recommend the combination of M05-2X/MG3S//X3LYP/6-31+G(2d,p) with a compromise between accuracy and efficiency for investigating larger water systems, which circumvents the bottleneck of MP2 or other high-level computations.

3.3 Numerical basis sets

In the case of numerical basis sets, the orbitals are truncated by a real-space cutoff parameter R_{cut}. For H_2O systems, the default "FINE" cutoff radius is 3.3 Å. Here, we tested a series of cutoff radii ($R_{cut} = 3, 4, 5, 6,$ and 7 Å) with the TNP basis set, and the computational results are listed in Table S2 and Table S3. The cutoff setting of 3.0 Å is insufficient to achieve converged results for the O–O separation and SE. For an accurate description of intermolecular hydrogen bonding interactions, one has to raise

the R_{cut} up to at least 5 Å. Hence, the following results were obtained by using $R_{cut} = 5$ Å, which yields rather satisfying results.

We also compared the O–O separation for $(H_2O)_n$ clusters with $n = 2$–10 computed from different methods (see Table S3). The O–O distances predicted by all these methods are rather close to each other. Compared with MP2/6-311++G(2d,2p) data, the RMSD of $\bar{R}_{O-O}$ from DNP and TNP computations are 0.056 and 0.039 Å, respectively, and the corresponding RMSD of relative energies for $(H_2O)_{4-10}$ isomers are 1.28 and 1.29 kcal/mol, respectively. Notably, the RMSD of $\bar{R}_{O-O}$ from TNP geometries is comparable to MG3S structures (0.034 Å).

Therefore, the numerical basis sets would be a good choice for investigating the structures of those more complicated systems, such as larger water clusters [131], and water clusters inside nanoscale confinements [37, 38], and so on, for which highly accurate calculations with large Gaussian basis sets are computationally prohibited.

4 Conclusions

In this work, we studied the geometric structures, stabilization energies, dipole moments, and vibrational frequencies of water clusters (from monomer to decamer) using the MP2 method and 11 widely used density functionals (M06-L, M05-2X, M06-2X, B3LYP, X3LYP, PBE0, BLYP, PBE, PBE1W, PW91, and LDA). The performance of different DFT functionals as well as the effects of basis sets (size, diffuse/polarization functions) was evaluated by a series of comparative computations. The most important findings can be summarized as follows:

1. As expected, the performance of LDA is seriously deficient. M05-2X is the best in describing binding energies of water clusters. PBE0 give relatively satisfying energies of $(H_2O)_n$ isomers with respect to the MP2 level, X3LYP yields a good geometry description and vibrational frequency prediction. The overall performance of hybrid functionals is typically better than the non-hybrid ones. Among those pure functionals, PBE1W performs better than the other three (PBE, PW91, and BLYP) in distinguishing the isomers of $(H_2O)_n$ ($n = 4$–10), whereas BLYP is reasonable in describing the structural properties of water clusters.

2. The split-valence basis set 6-31+G(2df,2p) is comparable to 6-311+G(2df,2p) for describing water clusters. Diffuse functions on oxygen atoms as well as d-polarization on oxygen and p-polarization on hydrogen are essential for achieving reasonable results. Adding more d-polarized functions on oxygen and

more p-polarized functions on hydrogen can further improve the description of water clusters. As a reasonable compromise between accuracy and efficiency, here we recommend the 6-31+(2d,p) basis set for describing the structures of larger water clusters or other complicated systems.

3. The combination of the pure GGA functional like PBE and the TNP numerical basis set, with $R_{cut} = 5.0$ Å, as implemented in the DMol^3 program, yields an acceptable structural description of the water clusters. Considering the high efficiency of the numerical basis set, such combination provides a practical choice for studying larger-sized $(H_2O)_n$ clusters, e.g., $n \geq 30$.

The scheme of M05-2X/MG3S//X3LYP/6-31+G(2d,p) stands out in depicting both geometries and energies of water clusters, which circumvents the bottleneck of high-level computations. Our results are intended to be used as a guide in choosing the computational methods most appropriate for studying the complicated hydrogen-bonded systems containing a large number of water molecules.

References

1. Ludwing R (2001) Angew Chem Int Ed 40:1808–1827
2. Ball P (2008) Chem Rev 108:74–108
3. Dyke TR (1977) J Chem Phys 66:492–497
4. Dyke TR, Mack KM, Muenter JS (1977) J Chem Phys 66:498–510
5. Odurola JA, Dyke TR (1980) J Chem Phys 72:5062–5070
6. Curtiss LA, Frurip DJ, Blander M (1979) J Chem Phys 71:2703–2711
7. Bentwood RM, Barnes AJ, Orville-Thomas WJ (1980) J Mol Spectrosc 84:391–404
8. Vernon MF, Krajnovich DJ, Kwok HS, Lisy JM, Sben YR, Lee YT (1982) J Chem Phys 77:47–57
9. Coker DF, Miller RE, Watts RO (1985) J Chem Phys 82:3554–3562
10. Wuelfert S, Herren D, Leutwyler S (1987) J Chem Phys 86:3751–3753
11. Engdahl A, Nelander B (1987) J Chem Phys 86:4831–4837
12. Knochenmuss R, Leutwyler S (1989) J Chem Phys 91:1268–1278
13. Pugliano N, Saykally RJ (1992) Science 257:1937–1940
14. Huisken F, Kaloudis M, Kulcke A (1996) J Chem Phys 104:17–25
15. Liu K, Brown MG, Carter C, Saykally RJ, Gregory JK, Clary DC (1996) Nature 381:501–503

16. Buck U, Ettischer I, Melzer M, Buch V, Sadlej J (1998) Phys Rev Lett 80:2578–2581
17. Brudermann J, Melzer M, Buck U, Kazimirski JK, Sadlej J, Buch V (1999) J Chem Phys 110:10649–10652
18. Gregory JK, Clary DC, Liu K, Brown MG, Saykally RJ (1997) Science 275:814–817
19. Goss LM, Sharpe SW, Blake TA, Vaida V, Brault JW (1999) J Phys Chem A 103:8620–8624
20. Sadlej J, Buch V, Kazimirski JK, Buck U (1999) J Phys Chem A 103:4933–4947
21. Kim KS, Dupuis M, Lie GC, Clementi E (1986) Chem Phys Lett 131:451–462
22. Kim K, Jordan KD (1994) J Phys Chem 98:10089–10094
23. Xantheas SS, Burnham CJ, Harrison RJ (2002) J Chem Phys 116:1493–1499
24. Anderson JA, Tschumper GS (2006) J Phys Chem A 110:7268–7271
25. Bryantsev VS, Diallo MS, van Duin ACT, Goddard WA (2009) J Chem Theory Comput 5:1016–1026
26. Kim J, Lee JY, Lee S, Mhin BJ, Kim KS (1995) J Chem Phys 102:310–317
27. Lee HM, Suh SB, Kim KS (2001) J Chem Phys 114:10749–10756
28. Xantheasas SS, Aprà E (2004) J Chem Phys 120:823–828
29. Estrin DA, Paglieri L, Corongiu G, Clementi E (1996) J Phys Chem 100:8701–8711
30. Batista ER, Xantheas SS, Jónsson H (1999) J Chem Phys 111:6011–6015
31. Kim KS, Mhin BJ, Choi U-S, Lee K (1992) J Chem Phys 97:6649–6662
32. Bilalbegović G (2010) J Phys Chem A 114:715–720
33. Partridge H, Schwenke DW (1997) J Chem Phys 106:4618–4639
34. Gordillo MC, Martí J (2000) Chem Phys Lett 329:341–345
35. Hummer G, Rasaiah JC, Noworyta JP (2001) Nature 414:188–190
36. Supriya S, Das SK (2003) J Cluster Sci 14:337–366
37. Wang L, Zhao JJ, Fang HP (2008) J Phys Chem C 112:11779–11785
38. Wang L, Zhao JJ, Li FY, Fang HP (2009) J Phys Chem C 113:5368–5375
39. Choi YC, Pak C, Kim KS (2006) J Chem Phys 124:094308-4
40. James T, Wales DJ, Rojas JH (2007) J Chem Phys 126:054506-13
41. Markovich G, Giniger R, Levin M, Cheshnovsky O (1993) Z Phys D 26:98–100
42. Xantheas SS, Dunning TH (1993) J Chem Phys 99:8774–8792
43. Xantheas SS (1996) J Phys Chem 100:9703–9713
44. Markovich G, Giniger R, Levin M, Cheshnovsky O (1991) Z Phys D 20:69–72
45. Xantheas SS (1995) J Am Chem Soc 117:10373–10380
46. Lee HM, Suh SB, Tarakeshwar P, Kim KS (2005) J Chem Phys 122:044306–044309
47. Kim KS, Tarakeshwar P, Lee JY (2000) Chem Rev 100:4145–4185
48. Gong X, Li J, Lu H, Wan R, Li J, Hu J, Fang H (2007) Nat Nanotechnol 2:709–712
49. Li J, Gong X, Lu H, Li D, Fang H, Zhou R (2007) Proc Natl Acad Sci 104:3687–3692
50. Gong X, Li J, Zhang H, Wan R, Lu H, Wang S, Fang H (2008) Phys Rev Lett 101:257801–257804
51. Tu Y, Xiu P, Wan R, Hu J, Zhou R, Fang H (2009) Proc Natl Acad Sci 106:18120–18124
52. Kim J, Kima KS (1998) J Chem Phys 109:5886–5895
53. Jensen JO, Krishnan PN, Burke LA (1996) Chem Phys Lett 260:499–506
54. Dahlke EE, Olson RM, Leverentz HR, Truhlar DG (2008) J Phys Chem A 112:3976–3984
55. Mhin BJ, Kim J, Lee S, Lee JY, Kim KS (1994) J Chem Phys 100:4484–4486
56. Bates DM, Tschumper GS (2009) J Phys Chem A 113:3555–3559
57. Qian J, Stöckelmann E, Hentschke R (1999) J Mol Model 5:281–286
58. Kabrede H, Hentschke R (2003) J Phys Chem B 107:3914–3920
59. James T, Wales DJ, Hernández-Rojas J (2005) Chem Phys Lett 415:302–307
60. Kiss PT, Baranyaia A (2009) J Chem Phys 131:204310–204314
61. Möller C, Plesset MS (1934) Phys Rev 46:618–622
62. Shields GC, Kirschner KN (2008) Synth React Inorg Met Org Nano Met Chem 38:32–39
63. Shields RM, Temelso B, Archer KA, Morrell TE, Shields GC (2010) J Phys Chem A 114:11725–11737
64. Sprik M, Hutter J, Parrinello M (1996) J Chem Phys 105:1142–1152
65. Sim F, Amant AS, Papai I, Salahub DR (1992) J Am Chem Soc 114:4391–4400
66. Pribble RN, Zwier TS (1994) Science 265:75–79
67. Gruenloh CJ, Carney JR, Arrington CA, Zwier TS, Fredricks SY, Jordan KD (1997) Science 276:1678–1681
68. Devlin JP, Joyce C, Buch V (2000) J Phys Chem A 104:1974–1977
69. Elstner M, Hobza P, Frauenheim T, Suhai S, Kaxiras E (2001) J Chem Phys 114:5149–5155
70. Tsuzuki S, Luthim HP (2001) J Chem Phys 114:3949–3957
71. Feibelman PJ (2002) Science 295:99–102
72. Supriya S, Manikumari S, Raghavaiah P, Das SK (2003) New J Chem 27:218–220
73. Michaelides A, Alavi A, King DA (2004) Phys Rev B 69:113401–113404
74. Černý J, Hobza P (2005) Phys Chem Chem Phys 7:1624–1626
75. Csonka GI, Ruzsinszky A, Perdrew JP (2005) J Phys Chem B 109:21471–21475
76. Ludwig R, Appelhagen A (2005) Angew Chem Int Ed 44:811–815
77. Zhao Y, Truhlar DG (2005) J Chem Theory Comput 1:415–432
78. Anderson JA, Hopkins BW, Chapman JL, Tschumper GS (2006) J Mol Struct Theochem 771:65–71
79. Kuo J-L, Kuhs WF (2006) J Phys Chem B 110:3697–3703
80. Todorova T, Seitsonen AP, Hutter J, Kuo I-FW, Mundy CJ (2006) J Phys Chem B 110:3685–3691
81. Bachrach SM (2008) J Phys Chem A 112:3722–3730
82. Dinescu A, Benson MT (2008) J Phys Chem A 112:12270–12280
83. Svozil D, Jungwirth P (2006) J Phys Chem A 110:9194–9199
84. McGrath MJ, Siepmann JI, Kuo I-FW, Mundy C (2006) Mol Phys 104:3619–3626
85. Zhao Y, Schultz NE, Truhlar DG (2006) J Chem Theory Comput 2:364–382
86. Zhao Y, Truhlar DG (2006) J Chem Phys 125:194101-18
87. Zhao Y, Truhlar DG (2008) J Chem Theory Comput 4:1849–1868
88. Zhao Y, Truhlar DG (2008) Theor Chem Account 120:215–241
89. Kim J, Majumdar D, Lee HM, Kim KS (1999) J Chem Phys 110:9128–9134
90. Császár AG (1995) J Mol Struct 346:141–152
91. Dahlke EE, Truhlar DG (2005) J Phys Chem B 109:15677–15683
92. Santra B, Michaelides A, Scheffler M (2007) J Chem Phys 127:184104-9
93. Lee HM, Suh SB, Lee JY, Tarakeshwar P, Kim KS (2000) J Chem Phys 112:9759–9772

94. Santra B, Michaelides A, Scheffler M (2009) J Chem Phys 131:124509-124517
95. Frisch MJ et al (2009) Gaussian 09, revision a. 02. Gaussian, Wallingford
96. Delley B (1990) J Chem Phys 92:508–517
97. Delley B (2000) J Chem Phys 113:7756–7764
98. Vosko SJ, Wilk L, Nusair M (1980) Can J Phys 58:1200–1211
99. Becke AD (1988) Phys Rev A 38:3098–3100
100. Perdew JP, Burke K, Ernzerhof M (1996) Phys Rev Lett 77:3865–3868
101. Perdew JP, Chevary JA, Vosko SH, Jackson KA, Pederson MR, Singh DJ, Fiolhais C (1992) Phys Rev B 46:6671–6687
102. Adamo C, Barone V (1999) J Chem Phys 110:6158–6170
103. Stephens PJ, Devlin FJ, Chabalowski CF, Frisch MJ (1994) J Phys Chem 98:11623–11627
104. Xu X, Goddard WA (2004) Proc Natl Acad Sci 101:2673–2677
105. Krishnan R, Binkley JS, Seeger R, Pople JA (1980) J Chem Phys 72:650–654
106. Purvis GD, Bartlett RJ (1982) J Chem Phys 76:1910–1918
107. Raghavachari K, Trucks GW, Pople JA, Head-Gordon M (1989) Chem Phys Lett 157:479–483
108. Watts JD, Gauss J, Bartlett RJ (1993) J Chem Phys 98:8718–8733
109. Werner H-L et al (2002) MOLPRO 2002, 6th edn. University of Birmingham, Birmingham
110. Boys SF, Bernardi D (1970) Mol Phys 19:553–566
111. Kozmutza C, Kryachko ES, Tfrist E (2000) J Mol Struct Theochem 501:435–444
112. Losada M, Leutwyler S (2002) J Chem Phys 117:2003–2012
113. Xu X, Goddard WA (2004) J Phys Chem A 108:2305–2313
114. Dyke TR, Muenter JS (1973) J Chem Phys 59:3125–3127
115. Tschumper GS, Leininger ML, Hoffman BC, Waleev EF, Schaefer HFI, Quack M (2002) J Chem Phys 116:690–701
116. Benedict WS, Gailar N, Plyler EK (1956) J Chem Phys 24:1139–1176
117. Fredin L, Nelander B, Ribbegard G (1977) J Chem Phys 66:4065–4068
118. Nelander B (1978) J Chem Phys 69:3870–3872
119. Scheiner AC, Baker J, Andzelm JW (1997) J Comput Chem 18:775–795
120. Hill J-R, Freeman CM, Delley B (1999) J Phys Chem A 103:3772–3777
121. Krishnan R, Pople JA (1978) Int J Quant Chem 14:91–100
122. Hall RJ, Hillier IH, Vincent MA (2000) Chem Phys Lett 320:139–143
123. Ramek M, Momany FA, Miller DM, Schäfer L (1996) J Mol Struct 375:189–191
124. Day MB, Kirschner KN, Shields GC (2005) J Phys Chem A 109:6773–6778
125. Nauta K, Miller RE (2000) Science 287:293–295
126. Campbell ES, Mezei M (1980) Mol Phys 41:883–905
127. Narten AH, Levy HA (1969) Science 165:447–454
128. Keutsch FN, Cruzan JD, Saykally RJ (2003) Chem Rev 103:2533–2577
129. Kim K, Jordan KD, Zwier TS (1994) J Am Chem Soc 116:11568–11569
130. Salvador P, Paizs B, Duran M, Suhai S (2001) J Comput Chem 22:765–786
131. Liu JJ, Wang L, Zhao JJ (2009) J Comput Theor Nanos 6:454–458